arXiv:1302.1241v1 [hep-th] 6 Feb 2013

Multi-centered Breathing Supersheets

Orestis Vasilakis

Department of Physics and Astronomy
University of Southern California
Los Angeles, CA 90089, USA

vasilaki@usc.edu

Abstract

We explore the multi-superthreads and supersheets solutions of six-dimensional $\mathcal{N} = 1$ supergravity coupled to a tensor multiplet. The solutions carry $D1$-$D5$-P charges, but no Kaluza-Klein monopole. We lay down the formalism to construct multi-centered supersheets with arbitrary and independent profiles. The solution is by construction free of Dirac stings in contrast to the five-dimensional construction where one has to separately solve integrability conditions. We explore this formalism to construct supersheets that fluctuate in both directions allowing a more general choice of profiles. These new solutions are genuinely six-dimensional, singular, fluctuating BPS solutions and by analyzing them we expect to learn more about the conjectured superstrata. We also derive the conditions under which different supersheets can touch, or even cross through each other.

Contents

1 Introduction 1

2 Superthreads and Supersheets 3
- 2.1 Multi-Superthreads 3
- 2.2 Multi-centered Supersheets 4

3 A Breathing Supersheet 6
- 3.1 The solution 7
- 3.2 Regularity and Asymptotic Charges 8

4 Multi-centered Breathers 10
- 4.1 The Solution 10
- 4.2 Regularity and Asymptotic Charges 12
- 4.3 Touching, Crossing & Regularity 13
- 4.4 Numerics on Global Regularity Conditions 16

5 Suggestions on the Addition of KKM 18

6 Conclusions 21

1 Introduction

A lot of work has recently been done in exploring BPS solutions of $\mathcal{N} = 1$ six-dimensional supergravity coupled to an anti-symmetric tensor multiplet. In [2], by exploring the results of [3, 4], it was shown that the BPS equations are linear. Linearity [5] of the BPS equations in five dimensions [6] has allowed the construction and classification of many three-charge solutions both supersymmetric [7, 8], and non-supersymmetric ones [9, 10, 11, 12, 13, 14, 15, 16, 17]. Consequently it is expected that the linearity of BPS equations in six dimensions will also allow such a classification for solutions that cannot be reduced to five dimensions.

Interest in solutions of six-dimensional supergravity was also raised by the conjectured superstrata, novel microstate geometries with three electric and three dipole magnetic charges that depend non-trivially in the compactification direction and thus are genuinely six dimensional. Finding smooth supergravity geometries with the same asymptotic charges as black holes is of central importance in the fuzzball proposal [18, 19, 20, 21, 22, 23, 24], which tries to explain the microscopic structure of black holes. Many of these microstates are expected to be exotic brane configurations which in general are non-geometric [25, 26]. However, in the D1-D5-P duality frame one of these configurations can admit a geometric description and thus it may also be smooth. It is expected that the superstratum, because of its additional fluctuation modes in the compactification direction, will contribute significantly to the microstates of three-charge geometries at a semiclassical level.

The existence of the superstratum was argued based on supersymmetry arguments in [27]. However its full description in terms of an exact supergravity solution is yet to be found. Some first steps towards that direction [1] along with the explicit construction of two and three charge solutions in six dimensions were done in [1, 2]. In [2] a one-dimensional D1-D5-P geometry with two dipole charges and arbitrary profile was constructed and named superthread. The linearity of the BPS equations was further explored in [1] to describe multiple superthreads with independent and arbitrary profiles. Upon smearing the multi superthread solutions give two-dimensional supersheet solutions that are in general characterized by profile functions of two variables. These solutions where found to be free of Dirac-strings without imposing any further constraints, in contrast to five-dimensional solutions where one writes the solution in terms of arbitrary electric and magnetic charges and then has to solve algebraic bubble equations that relate the charges and the positions of the objects. For a specific choice of profile functions the smearing integrals were performed to find a single center supersheet solution with trivial reduction to five dimensions [29, 30, 31].

Here we generalize the results of [1] by considering multi-centered breathing supersheet solutions that after smearing depend non-trivially in the compactification direction and are thus genuinely six-dimensional. They are breathing states because the shape of the configuration is fixed but its scale varies with the compactification direction. They represent a new class of six-dimensional solutions that are by construction free of Dirac-strings. In five dimensions the cancellation of Dirac strings is given by integrability conditions which for single-centered objects appear as a radius relation that give the position of the object in terms of its charges, while for multi-centered objects they express the interactions between the centers in terms of magnetic fluxes. Thus it is interesting to explore how these interactions get embedded in the solution in the six-dimensional geometry and allow us in the future to construct multi-centered microstate geometries in six dimensions. Analyzing the structure of these objects will also help us understand more about the superstratum which is also a genuine six-dimensional geometry. A novel feature of these new geometries is that, because of their fluctuation in the sixth dimension, under certain conditions they can touch or even cross through each other.

In section 2 we briefly summarize the main results of [1] and extend the formalism to describe multi-centered supersheets. In section 3 for a specific choice of profile functions we calculate the smearing integrals to construct an axisymmetric breathing supersheet, with an arbitrary periodic function describing the fluctuations in the compact direction. We further examine the asymptotic charges of the solution and the restrictions put on this arbitrary function by the absence of closed timelike curves. In section 4 we generalize the results of section 3 to construct multi-centered axisymmetric breathing supersheets with independent and arbitrary oscillation profiles along the compact direction. We derive the local conditions that need to be satisfied for two supersheets to touch or cross and by a specific choice of examples we provide a numerical analysis of the global conditions as well. In section 5, based on results of section 3, we give general arguments about the structure of six-dimensional solutions and a possible perturbative approach towards constructing black geometries as well as the superstratum. Finally we display our conclusions in section 6.

---

[1] A different perturbative approach towards the superstratum based on string amplitudes has recently been given in [28].

2 Superthreads and Supersheets

In this section we describe superthreads and a supersheets by reviewing the main results of [1] and providing some simple generalizations. The six-dimensional metric is

$$ds^2 = 2H^{-1}(dv + \beta)\left(du + \omega + \frac{\mathcal{F}}{2}(dv + \beta)\right) - H ds_4^2 \tag{2.1}$$

The four-dimensional base metric satisfies some special conditions that will not be relevant here since we are simply going to take ds_4^2 to be the flat metric on $\mathbb{R}^4$. The coordinate v has period L and the metric functions in general depend on both v and the $\mathbb{R}^4$ coordinates $\vec{x}$. We want to describe 1/8-BPS geometries that have D1-D5-P charges. For simplicity we choose $\beta = 0$, which means that there will be no Kaluza-Klein monopoles in the solution. In addition to that, because $\beta = 0$, although the inhomogeneous terms in the BPS equations [1] contain v derivatives, the differential operators in the left hand side contain no v derivatives. The latter means that because of linearity the solutions we find, although v-dependent, they can be thought to be assembled by constant v sections of the full solution.

2.1 Multi-Superthreads

The solutions consist of supersymmetric one-dimensional threads (hence superthreads) that run across the v coordinate. The shape of the superthreads is given by profile functions $\vec{F}(v)$. In [1] the BPS equations were solved to describe multi-superthread solutions with independent and arbitrary shapes (fig.1). The solution contains non-trivial shape-shape interaction terms which disappear when all the superthreads are parallel to each other.

Defining $H = \sqrt{Z_1 Z_2}$ with Z_1,Z_2 harmonic functions that encode the $D1$, $D5$ charges respectively and denoting by $\vec{F}_p(v)$ the profile function of the pth thread, the multi-superthread solution has constituent parts

$$\begin{aligned}
Z_i &= 1 \ + \ \sum_{p=1}^{n} \frac{Q_{i\,p}}{|\vec{x} - \vec{F}^{(p)}(v)|^2} \\
\mathcal{F} \ &= \ -4 \ - \ 4\sum_{p=1}^{n} \frac{Q_{3\,p}}{R_p^2} \ - \ \frac{1}{2} \sum_{p,q=1}^{n} \frac{(Q_{1p}Q_{2q} + Q_{2p}Q_{1q})}{R_p^2 R_q^2} \left(\dot{\vec{F}}^{(p)} \cdot \dot{\vec{F}}^{(q)}\right) + \\
&+ \ \sum_{\substack{p,q=1 \\ p \neq q}}^{n} (Q_{1p}Q_{2q} + Q_{2p}Q_{1q}) \frac{1}{R_p^2 R_q^2} \frac{\dot{F}_i^{(p)} \, \dot{F}_j^{(q)} \, \mathcal{A}_{ij}^{(p,q)}}{\left|\vec{F}^{(p)} - \vec{F}^{(q)}\right|^2} \\
\omega &= \omega_0 + \omega_1 + \omega_2 \\
\omega_0 \ &= \ \sum_{i=1}^{2} \sum_{p=1}^{n} \frac{Q_{i\,p} \, \dot{F}_m^{(p)} dx^m}{|\vec{x} - \vec{F}^{(p)}(v)|^2} \\
\omega_1 \ &= \ \frac{1}{2} \sum_{p,q=1}^{n} (Q_{1\,p} \, Q_{2\,q} + Q_{2\,p} \, Q_{1\,q}) \frac{\dot{F}_m^{(p)} dx^m}{R_p^2 \, R_q^2} \\
\omega_2 \ &= \ \frac{1}{4} \sum_{\substack{p,q=1 \\ p \neq q}}^{n} (Q_{1p}Q_{2q} + Q_{2p}Q_{1q}) \frac{\left(\dot{F}_i^{(p)} - \dot{F}_i^{(q)}\right)}{\left|\vec{F}^{(p)} - \vec{F}^{(q)}\right|^2} \left\{ \left(\frac{1}{R_p^2} - \frac{1}{R_q^2} \right) dx^i \ - \ \frac{2}{R_p^2 R_q^2} \, \mathcal{A}_{ij}^{(p,q)} \, dx^j \right\}
\end{aligned}$$

where in the above we used the notation $\partial_v \Phi = \dot{\Phi}$. Also we required that $Z_i \to 1$ at infinity so that the metric is asymptotically Minkowskian and we define

$$\begin{aligned}
&\vec{R}_p = \vec{x} - \vec{F}_p \\
&\mathcal{A}_{ij}^{(p,q)} \ \equiv \ R_i^{(p)} R_j^{(q)} - R_j^{(p)} R_i^{(q)} \ - \ \varepsilon^{ijk\ell} R_k^{(p)} R_\ell^{(q)}
\end{aligned} \tag{2.2}$$

with $\varepsilon^{1234} = 1$. The anti-self-dual twoform area element $\mathcal{A}_{ij}^{(p,q)}$ encodes the non-trivial interactions between non-parallel superthreads.

2.2 Multi-centered Supersheets

In the continuum limit the summations are promoted to integrals and the indices p, q become continuous variables σ_1, σ_2. The objects that occur after smearing are two-dimensional geometries which are called supersheets (fig.1). The continuum limit for a single supersheet was considered in [1]. Here we give the immediate generalization for multi-centered supersheets with arbitrary and independent two-dimensional profiles. Thus for a multi-centered solution the profile functions $\vec{F}_p(v)$ become functions of two variables $\vec{F}_I(\sigma^{(I)}, v)$ and the discrete charges Q_{ip} are being replaced

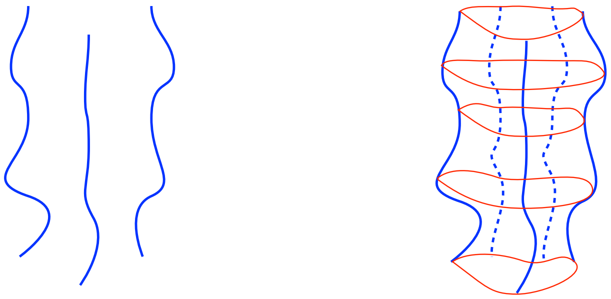

Figure 1: *Multi-superthread solution with independent profile functions* $\vec{F}_p(v)$ *for each thread.. After smearing the supersheet is described by generic functions of two variables* $\vec{F}(\sigma, v)$*.*

by density functions $\rho^{(I)}(\sigma^{(I)})$. In the above we used capital latin indices to separate between different centers of the solution. Then we have

$$
\begin{aligned}
Z_i &= 1 \; + \; \sum_I \int_0^{2\pi} \frac{\rho_i^{(I)}(\sigma^{(I)})\, d\sigma^{(I)}}{|\vec{x} - \vec{F}_I(\sigma^{(I)}, v)|^2} \\
\mathcal{F} \;&=\; -4 \;-\; \sum_I 4 \int_0^{2\pi} \frac{\rho_3^{(I)}(\sigma^{(I)})}{R^{(I)}(\sigma^{(I)})^2}\, d\sigma^{(I)} \\
&- \sum_{I,J} \int_0^{2\pi} \int_0^{2\pi} \left(\rho_1^{(I)}(\sigma_1^{(I)})\rho_2^{(J)}(\sigma_2^{(J)}) + \rho_2^{(I)}(\sigma_1^{(I)})\rho_1^{(J)}(\sigma_2^{(J)})\right) \frac{1}{R^{(I)}(\sigma_1^{(I)})^2 R^{(J)}(\sigma_2^{(J)})^2} \\
&\left[\frac{1}{2} \left(\partial_v \vec{F}_I(\sigma_1^{(I)}, v)\right) \cdot \left(\partial_v \vec{F}_J(\sigma_2^{(J)}, v)\right) \;-\; \frac{\partial_v F_{I,i}(\sigma_1^{(I)}, v)\, \partial_v F_{J,j}(\sigma_2^{(J)}, v) \;\; \mathcal{A}_{ij}^{(IJ)}(\sigma_1^{(I)}, \sigma_2^{(J)})}{\left|\vec{F}_I(\sigma_1^{(I)}, v) - \vec{F}_J(\sigma_2^{(J)}, v)\right|^2} \right] d\sigma_1^{(I)} d\sigma_2^{(J)} \\
\omega_0 \;&=\; \sum_I \sum_{i=1}^{2} \int_0^{2\pi} \frac{\rho_i^{(I)}(\sigma^{(I)})\, \partial_v \vec{F}_I(\sigma^{(I)}, v) \cdot d\vec{x}}{|\vec{x} - \vec{F}_I(\sigma^{(I)}, v)|^2}\, d\sigma^{(I)} \\
\omega_1 \;&=\; \frac{1}{2} \sum_{I,J} \int_0^{2\pi} \int_0^{2\pi} \frac{\left(\rho_1^{(I)}(\sigma_1^{(I)})\rho_2^{(J)}(\sigma_2^{(J)}) + \rho_2^{(I)}(\sigma_1^{(I)})\rho_1^{(J)}(\sigma_2^{(J)})\right)\partial_v \vec{F}_I(\sigma_1^{(I)}, v) \cdot d\vec{x}}{R^{(I)}(\sigma_1^{(I)}, v, \vec{x})^2\, R^{(J)}(\sigma_2^{(J)}, v, \vec{x})^2}\, d\sigma_1^{(I)} d\sigma_2^{(J)} \\
\omega_2 \;&=\; \frac{1}{4} \sum_{I,J} \int_0^{2\pi} \int_0^{2\pi} \left(\rho_1^{(I)}(\sigma_1^{(I)})\rho_2^{(J)}(\sigma_2^{(J)}) + \rho_2^{(I)}(\sigma_1^{(I)})\rho_1^{(J)}(\sigma_2^{(J)})\right) \frac{\left(\partial_v F_{I,i}(\sigma_1^{(I)}, v) - \partial_v F_{J,i}(\sigma_2^{(J)}, v)\right)}{\left|\vec{F}_I(\sigma_1^{(I)}, v) - \vec{F}_J(\sigma_2^{(J)}, v)\right|^2} \\
&\left\{ \left(\frac{1}{R^{(I)}(\sigma_1^{(I)})^2} - \frac{1}{R^{(J)}(\sigma_2^{(J)})^2} \right) dx^i \;-\; \frac{2}{R^{(I)}(\sigma_1^{(I)})^2 R^{(J)}(\sigma_2^{(J)})^2}\, \mathcal{A}_{ij}^{IJ}(\sigma_1^{(I)}, \sigma_2^{(J)})\, dx^j \right\} d\sigma_1^{(I)} d\sigma_2^{(J)}
\end{aligned}
\tag{2.3}
$$

where we define

$$
\begin{aligned}
\vec{R}^{(I)}(\sigma^{(I)}) \;&\equiv\; \vec{x} \;-\; \vec{F}_I(\sigma^{(I)}, v) \\
\mathcal{A}_{ij}^{IJ}(\sigma_1^{(I)}, \sigma_2^{(J)}) \;&\equiv\; R_i^{(I)}(\sigma_1^{(I)})R_j^{(J)}(\sigma_2^{(J)}) - R_j^{(I)}(\sigma_1^{(I)})R_i^{(J)}(\sigma_2^{(J)}) \;-\; \varepsilon^{ijk\ell} R_k^{(I)}(\sigma_1^{(I)})R_\ell^{(J)}(\sigma_2^{(J)})
\end{aligned}
\tag{2.4}
$$

The capital latin indices in the integration variables $\sigma_i^{(I)}$ of (2.3), (2.4) are dummy indices and can be removed. For the single integrals this is a trivial observation, while for the double integrals it is based on the symmetry of the integrand in exchanging $I \leftrightarrow J$. The structure of the equations (2.3) indicates that a multi-centered supersheet solution will consist of two parts. First, there will be a summation over single-centered supersheets of different radii and profiles coming from single summation terms and from double summations when $I = J$. Secondly there will be interaction terms between the different supersheets coming from double summations when $I \neq J$. Furthermore, because superthreads interact in pairs so will the resulting supersheets. Thus the solution naturally decomposes as

$$\begin{aligned}
Z_i &= 1 + \sum H_i^{(I)} \\
\omega &= \sum_I \omega^{(I)} + \sum_{I \neq J} \omega^{(I,J)} \\
\mathcal{F} &= -4 + \sum_I \mathcal{F}^{(I)} + \sum_{I \neq J} \mathcal{F}^{(I,J)}
\end{aligned} \tag{2.5}$$

Because the integrands of ω_2 and $\mathcal{F}$ are symmetric in exchanging $I \leftrightarrow J$, we have $\omega_2^{(I,J)} = \omega_2^{(J,I)}$ and $\mathcal{F}^{(I,J)} = \mathcal{F}^{(J,I)}$. So we can further reduce (2.5) to

$$\begin{aligned}
Z_i &= 1 + \sum H_i^{(I)} \\
\omega &= \sum_I \omega^{(I)} + \sum_{I<J} \left(\omega_1^{(I,J)} + \omega_1^{(J,I)} + 2\omega_2^{(I,J)} \right) \\
\mathcal{F} &= -4 + \sum_I \mathcal{F}^{(I)} + 2 \sum_{I<J} \mathcal{F}^{(I,J)}
\end{aligned} \tag{2.6}$$

3 A Breathing Supersheet

In [1] by considering superthreads of helical profile the smearing integrals for a single-centered supersheet were explicitly calculated. Although the profile functions depended on both v and σ the resulting supersheet was independent of v and it matched a special class of already known five-dimensional solutions [29], [30], [31]. Here we want to extend these results by considering a slightly more general choice of profile functions so that the resulting supersheet can also fluctuate in the coordinate v. Thus we choose

$$\vec{F}(v,\sigma) = (A(\lambda v) cos(\kappa v + \sigma)\,,\, A(\lambda v) sin(\kappa v + \sigma)\,,\, 0\,,\, 0) \tag{3.1}$$

as in [1] we once again choose helical profile functions, but now the radius A instead of being constant is an arbitrary function of v. The resulting supersheet would have a circular profile in $\mathbb{R}^4$ for a specific value of v, with varying circle radius as we move along the v direction. The constants

λ and κ are of the form $2\pi n/L$, where n is an integer, and can in principle be independent. Although our results are given for a circular profile we believe that they can be generalized to any closed non-intersecting curve by constructing the appropriate Green's functions.
For the $\mathbb{R}^4$ base space with take double polar coordinates

$$x_1 = \eta cos\psi\,,\, x_2 = \eta sin\psi\,,\, x_3 = \zeta cos\phi\,,\, x_4 = \zeta sin\phi \tag{3.2}$$

from which we can go to spherical coordinates by substituting

$$\eta = r sin\theta\,,\, \zeta = r cos\theta \tag{3.3}$$

3.1 The solution

To describe a single supersheet we need to calculate the integrals (2.3) with no summations and the latin indices removed. We also consider a constant charge distribution

$$\rho_i(\sigma) = \frac{Q_i}{2\pi} \tag{3.4}$$

The integrals are easily calculated by going to the complex plane and summing the residues of the poles that are within the unit circle. The double integrals transform to a double complex integral and the residues of the first complex integration act as integrand functions for the second complex integral. Then for the functions describing the solution we find

$$Z_1 = 1 + \frac{Q_1}{\Sigma}\,,\, Z_2 = 1 + \frac{Q_2}{\Sigma} \tag{3.5}$$

where

$$\Sigma = \sqrt{(A^2+\eta^2+\zeta^2)^2 - 4A^2\eta^2} = \sqrt{(A^2+r^2)^2 - 4A^2r^2sin^2\theta} \tag{3.6}$$

is the position of the supersheet in $\mathbb{R}^4$ and is now v dependent via the function $A(\lambda v)$
Similarly we have.

$$\mathcal{F} = -4 - \frac{4Q_3A^2 - Q_1Q_2\left(\lambda^2\acute{A}^2 + \kappa^2A^2\right)}{A^2\Sigma} - Q_1Q_2\frac{\left(\lambda^2\acute{A}^2 + \kappa^2A^2\right)(\eta^2+\zeta^2)}{A^2\Sigma^2} \tag{3.7}$$

and for the angular momentum one obtains

$$\begin{aligned}\omega = \frac{(Q_1+Q_2)}{2\eta A}\left(-1 + \frac{A^2+\eta^2+\zeta^2}{\Sigma}\right)\left(\kappa A\eta d\psi + \lambda\acute{A}d\eta\right) + \\ + Q_1Q_2\frac{\eta}{A\Sigma^2}\left(\eta\kappa A d\psi + \lambda\acute{A}d\eta\right) + Q_1Q_2\frac{\zeta}{A\Sigma^2}\left(\zeta\kappa A d\phi + \lambda\acute{A}d\zeta\right)\end{aligned} \tag{3.8}$$

where

$$\partial_v A = \dot{A} = \acute{A}\lambda \tag{3.9}$$

It is interesting to observe that the functions (3.7) and (3.8) describing the helical breather, because of linearity of the BPS equations, can be considered as the superposition of two distinct cases of supersheets: one made from superthreads of helical profile with constant radius ($\lambda = 0$) and another made of straight superthreads with a breathing profile of ($\kappa = 0$). Thus breathing and helical modes of the solution are independent, originating from the fact that the profile function factorizes and each mode is sourced by a different factor of (3.1).

The coordinates of $\mathbb{R}^4$ in which the angular momentum one form ω has legs depends from $\dot{F}_i dx^i$, (2.3). Thus the helical mode generates the components $d\psi$ and $d\phi$. The breathing mode generates new components $d\eta$ and $d\zeta$ along radial directions, expressing that the $\mathbb{R}^4$ circular profile changes radius as we move along v.

3.2 Regularity and Asymptotic Charges

Before examining our solution for closed timelike curves there are some restrictions to be placed on the function A. In general there is the possibility of antidiametric points of the $\mathbb{R}^4$ circular profile to cross over each other at specific values of $v = v_0$. For our choice of profile functions this happens exactly when $A(\lambda v_0) = 0$. Then the functions $\mathcal{F}$ and ω diverge. Thus we need

$$A(\lambda v) \neq 0 \quad \forall v \in [0, L] \tag{3.10}$$

For example for the simple choice $A = b + acos(\lambda v)$ we need $b > a$. However, since A is a periodic function of v there will be points $v = v_1$ such that $\dot{A}(\lambda v_1) = 0$. For these values of v the solution and its physical analysis exactly matches that of [1] where A is constant. That might lead to an interesting perturbative approach in exploring the superstratum by expanding around the points $\dot{A}(\lambda v_1) = 0$ where the superstratum should match the v-independent supertube solution. Thus the superstratum can possibly be realized as additional perturbation modes in the supertube solution around these points. We further comment on this idea in section 5. A different perturbative approach to the superstratum [2] has recently appeared in [28].

We read the asymptotic charges of the solution from the expansion of Z_1, Z_2, $\mathcal{F}$ and ω for $r \to \infty$. The asymptotic electric charges are

$$Q_{1,\infty} = Q_1\,,\; Q_{2,\infty} = Q_2\,,\; Q_{3,\infty} = Q_3 \tag{3.11}$$

and from the expansion of ω we get

$$\omega \sim \frac{1}{r^2}\left(\left(\kappa A^2(Q_1+Q_2) + \kappa Q_1 Q_2\right) sin^2\theta d\psi + \kappa Q_1 Q_2 cos^2\theta d\phi + \frac{1}{2}(Q_1+Q_2)\lambda A\dot{A} sin(2\theta) d\theta\right) \tag{3.12}$$

---

[2] The superstratum discussed in [28] is also different since it would be a generalization of the three electric one magnetic dipole charge supertube presented in [32].

thus, in contrast to the case that the supersheet is v independent there is an additional term proportional to $\dot{A}$ along the θ direction.

To examine the solution for closed timelike curves it is useful to rewrite the metric (2.1) by completing the squares

$$ds^2 = H^{-1}\mathcal{F}\left(dv + \beta + \mathcal{F}^{-1}(du+\omega)\right)^2 - H^{-1}\mathcal{F}^{-1}\left(du+\omega\right)^2 - Hds_4^2 \tag{3.13}$$

Taking a slice of u =constant the absence of closed timelike curves requires that the following conditions hold globally

$$\mathcal{F} \leq 0 \tag{3.14}$$

$$ds_4^2 + \frac{\omega^2}{H^2\mathcal{F}} \geq 0 \tag{3.15}$$

From (3.14) for $r \to 0$ we get

$$Q_3 \geq \frac{Q_1Q_2\left(\lambda^2\acute{A}^2 + \kappa^2A^2\right)}{4A^2} \tag{3.16}$$

the charge Q_3 should be big enough so that is greater than the right hand side of (3.16) for every value of v. Since Q_3 enters $\mathcal{F}$ as a harmonic term, the charge Q_3 can be an arbitrary function of v without affecting the solution. Consequently by defining

$$Q_3(v) = \widehat{Q}_3\frac{\left(\lambda^2\acute{A}^2 + \kappa^2A^2\right)}{\kappa^2A^2} \tag{3.17}$$

we get a result similar to the five dimensional case examined in [1]

$$\widehat{Q}_3 \geq \frac{1}{4}\kappa^2Q_1Q_2 \tag{3.18}$$

where $\widehat{Q}_3$ is an effective v-independent charge. From (3.15) by taking the near supersheet limit $\Sigma \to 0$ we obtain from the leading order term

$$\frac{1}{\kappa^2A^2 + \lambda^2\acute{A}^2}\left(A\kappa dr - \acute{A}\lambda r sin^2\theta d\psi - \acute{A}\lambda r cos^2\theta d\phi\right)^2 + r^2sin^2\theta cos^2\theta\left(d\psi + d\phi\right)^2 + rd\theta^2 \tag{3.19}$$

which is always positive. Suppose we have $\dot{A}(\lambda v_1) = 0$ at some point v_1, then we can make the leading order term vanish by choosing, consistently with the $\Sigma \to 0$ limit, $r \to A$, $\theta \to \pi/2$. By considering the next to leading order term in the expansion we get the constraint given in [1] for a non-breathing supersheet.

$$Q_1Q_2\left(\widetilde{Q}_3(v_1) - \frac{1}{4}\kappa^2A(\lambda v_1)(Q_1+Q_2)\right) \geq 0 \tag{3.20}$$

thus

$$\widetilde{Q}_3(v_1) \geq \frac{1}{4}\kappa^2A(\lambda v_1)(Q_1+Q_2) \tag{3.21}$$

where we defined

$$\widetilde{Q}_3(v) = Q_3 - \frac{Q_1 Q_2 \left(\lambda^2 \acute{A}^2 + \kappa^2 A^2\right)}{4A^2} \tag{3.22}$$

Also at the limit $\Sigma \to 0$ the metric function blows up and thus the breathing supersheet geometry is singular. This is consistent with the five-dimensional non-breathing supersheet picture and the comment in the beginning of section 2 that because $\beta = 0$ these geometries can be thought as a collection of slices with $v =$constant. Thus for every value of v we have a singularity with radial profile in $\mathbb{R}^4$ and the collections of all the different v-slices creates a singular six-dimensional geometry.

4 Multi-centered Breathers

Here we calculate the smearing integrals (2.3) for multi-centered breathing supersheets. Generalizing (3.1) we separate the superthreads at different sets A_I with profile functions at each set

$$\vec{F}_I(v, \sigma^{(I)}) = (A_I(\lambda_I v) cos(\kappa_I v + \sigma^{(I)})\,,\, A_1(\lambda_I v) sin(\kappa_I v + \sigma^{(I)})\,,\, 0\,,\, 0) \tag{4.1}$$

with $A_I < A_J$ for $I < J \quad \forall v \in [0, L]$.
To each set of threads we give a constant charge distribution given by

$$\rho_i^{(I)}(\sigma^{(I)}) = \frac{Q_i^{(I)}}{2\pi} \tag{4.2}$$

4.1 The Solution

These supersheets have circular profiles in $\mathbb{R}^4$ with radii $A_I(\lambda_I v)$ which fluctuate as we move along the v coordinate. In general they are also non-parallel as each one has its own function $A_I(\lambda_I v)$ that oscillates along v. By using (2.6) we write the solution as a combination of single-centre and interaction terms. For the singe-centre terms we have

$$\begin{aligned}
H_i^{(I)} &= \frac{Q_i^{(I)}}{\Sigma_I} \\
\mathcal{F}^{(I)} &= -\frac{4Q_3^{(I)} A_I^2 - Q_1^{(I)} Q_2^{(I)} \left(\lambda_I^2 \acute{A}_I^{\,2} + \kappa_I^2 A_I^2\right)}{A_I^2 \Sigma_I} - Q_1^{(I)} Q_2^{(I)} \frac{\left(\lambda_I^2 \acute{A}_I^{\,2} + \kappa_I^2 A_I^2\right)(\eta^2 + \zeta^2)}{A_I^2 \Sigma_I^2} \\
\omega^{(I)} &= \frac{(Q_1^{(I)} + Q_2^{(I)})}{2\eta A_I} \left(-1 + \frac{A_I^2 + \eta^2 + \zeta^2}{\Sigma_I}\right) \left(\kappa_I A_I \eta d\psi + \lambda_I \acute{A}_I d\eta\right) + \\
&+ Q_1^{(I)} Q_2^{(I)} \frac{\eta}{A_I \Sigma_I^2} \left(\eta \kappa_I A_I d\psi + \lambda_I \acute{A}_I d\eta\right) + Q_1^{(I)} Q_2^{(I)} \frac{\zeta}{A_I \Sigma_I^2} \left(\zeta \kappa_I A_I d\phi + \lambda_I \acute{A}_I d\zeta\right)
\end{aligned} \tag{4.3}$$

and for the interaction terms

$$\begin{aligned}
\mathcal{F}^{(I,J)} &= -\frac{4Q_3^{(I,J)}}{\Sigma_I} - \frac{Q_1^{(I)}Q_2^{(J)} + Q_2^{(I)}Q_1^{(J)}}{2}\left(\lambda_I\lambda_J\acute{A}_I\acute{A}_J + \kappa_I\kappa_J A_I A_J\right)\left(-\frac{1}{A_I A_J \Sigma_I} + \frac{\eta^2+\zeta^2}{A_I A_J \Sigma_I \Sigma_J}\right)\\
\omega_1^{(I,J)} &= \frac{Q_1^{(I)}Q_2^{(J)} + Q_2^{(I)}Q_1^{(J)}}{4\eta A_J \Sigma_I \Sigma_J}\left(A_J^2 + \eta^2 + \zeta^2 - \Sigma_J\right)\left(\kappa_J A_J \eta d\psi + \lambda_J \acute{A}_J d\eta\right)\\
\omega_2^{(I,J)} &= \left(Q_1^{(I)}Q_2^{(J)} + Q_2^{(I)}Q_1^{(J)}\right)\Bigg(\left(-G_1^{(I,J)}\kappa_I + G_2^{(I,J)}\kappa_J\right)d\psi+\\
&+\left(-\frac{\acute{A}_I}{A_I\eta}G_1^{(I,J)}\lambda_I + \frac{\acute{A}_J}{A_J\eta}G_2^{(I,J)}\lambda_J\right)d\eta+\\
&+\left(L_1^{(I,J)}A_I A_J(\kappa_I+\kappa_J) + L_2^{(I,J)}(\kappa_I A_I^2 + \kappa_J A_J^2)\right)d\phi+\\
&+\frac{1}{\zeta}\left(L_1^{(I,J)}(\lambda_I A_J \acute{A}_I + \lambda_J A_I \acute{A}_J) + L_2^{(I,J)}(\lambda_I A_I \acute{A}_I + \lambda_J A_J \acute{A}_J)\right)d\zeta\Bigg)
\end{aligned} \tag{4.4}$$

where, as in (2.6) we require $I < J$ and we also define

$$\Sigma_I = \sqrt{(A_I^2 + \eta^2 + \zeta^2)^2 - 4A_I^2\eta^2} = \sqrt{(A_I^2 + r^2)^2 - 4A_I^2 r^2 sin^2\theta} \tag{4.5}$$

and we have introduced the functions

$$\begin{aligned}
G_1^{(I,J)} &= \frac{(A_I^2 + \Sigma_J + \zeta^2)(A_I^2 - \Sigma_I + \zeta^2) + \eta^2(2\zeta^2 - 2A_I^2 + \Sigma_J - \Sigma_I) + \eta^4}{8(A_I^2 - A_J^2)\Sigma_I\Sigma_J}\\
G_2^{(I,J)} &= \frac{A_J^4 + 2A_I^2\Sigma_J - (\Sigma_I - \eta^2 - \zeta^2)(\Sigma_J + \eta^2 + \zeta^2) - A_J^2(\Sigma_I + \Sigma_J + 2\eta^2 - 2\zeta^2)}{8(A_I^2 - A_J^2)\Sigma_I\Sigma_J}\\
L_1^{(I,J)} &= \frac{A_I A_J \zeta^2\left(A_I^2(\Sigma_J - 2\eta^2) + (\Sigma_I + \Sigma_J)(\eta^2 + \zeta^2) + A_J^2(\Sigma_I + 2\eta^2)\right)}{(A_I^2 - A_J^2)\Sigma_I\Sigma_J(A_J^2 - A_I^2 + \Sigma_I + \Sigma_J)(A_I^2(\Sigma_J - \eta^2 - \zeta^2) + A_J^2(\Sigma_I + \eta^2 + \zeta^2))}\\
L_2^{(I,J)} &= \frac{\zeta^2\left((A_I^2 - A_J^2)\Sigma_I\Sigma_J - (A_I^2 + A_J^2)(A_I^2 + \eta^2 + \zeta^2)\Sigma_J\right)}{2(A_I^2 - A_J^2)\Sigma_I\Sigma_J(A_J^2 - A_I^2 + \Sigma_I + \Sigma_J)(A_I^2(\Sigma_J - \eta^2 - \zeta^2) + A_J^2(\Sigma_I + \eta^2 + \zeta^2))}-\\
&-\frac{\zeta^2\left((A_J^2 + \eta^2 + \zeta^2)\left(A_J^2(\Sigma_I + \eta^2 + \zeta^2) + A_I^2(A_J^2 + \Sigma_I - \eta^2 - \zeta^2) - A_I^4\right)\right)}{2(A_I^2 - A_J^2)\Sigma_I\Sigma_J(A_J^2 - A_I^2 + \Sigma_I + \Sigma_J)(A_I^2(\Sigma_J - \eta^2 - \zeta^2) + A_J^2(\Sigma_I + \eta^2 + \zeta^2))}
\end{aligned} \tag{4.6}$$

Although the integrands of the interaction terms $\omega_2^{(I,J)}$ and $\mathcal{F}^{(I,J)}$ are symmetric under $I \leftrightarrow J$, the functions that occur after smearing are not. This is due to the fact that while calculating the integrals we had to made use of $A_I < A_J$ for $I < J$. Our solutions match the already studied five-dimensional solutions provided we set all $\lambda_I = 0$. In the five-dimensional case however one writes down the solution with freely adjustable parameters and positions and the interaction terms are symmetric under $I \leftrightarrow J$. Then one has to separately solve integrability conditions (also called bubble equations), coming from requiring the absence of Dirac strings, that relate the positions of the objects with their electric and magnetic dipole charges. Here the solution is by construction free of Dirac strings and that is reflected in the lack of symmetry under $I \leftrightarrow J$.

To this end it is useful to provide additional details on how the asymmetry in $I \leftrightarrow J$ arises from the multi-centered integrals (2.3). To calculate any double integral expressing the interactions between the centers I and J we go to the complex plane by introducing complex variables $z = e^{i\sigma_1}$, $w = e^{i\sigma_2}$. We perform a double complex integration where the residues of the first integral become the integrand of the second. At each integral we pick the poles that are within the unit circle. The denominator of the integrand contains the factor $(A_I z - A_J w)(A_J z - A_I w)$, coming from the term $|\vec{F}_I(\sigma_1, v) - \vec{F}_J(\sigma_2, v)|^2$ in (2.3). As a result when performing the first integral (either over z or w) we need to know which of the two ratios $\frac{A_I}{A_J}$ or $\frac{A_J}{A_I}$ is less than one, to pick the pole within the unit circle, and thus the ordering of the supersheets matters.

4.2 Regularity and Asymptotic Charges

Once again we have to verify that our solution is free of closed timelike curves (3.14), (3.15). For each of the single-centered terms of the solution the analysis of section 3.2 can be repeated in exactly the same manner and the conditions (3.14) and (3.15) give exactly the conditions (3.16) - (3.22) with the capital latin index I included to specify the center we are referring to. In the multi-centered case though one has to examine the interaction terms as well. Imposing

$$\mathcal{F}^{(I,J)} \leq 0 \tag{4.7}$$

we get from (4.4) the additional constraint

$$Q_3^{(I,J)} \geq \left(Q_1^{(I)} Q_2^{(J)} + Q_2^{(I)} Q_1^{(J)} \right) \frac{\lambda_I \lambda_J \acute{A}_I \acute{A}_J + \kappa_I \kappa_J A_I A_J}{8 A_I A_J} \tag{4.8}$$

Similarly to (3.17) we can define an effective v-independent interaction charge $\widehat{Q}_3^{(I,J)}$ such that,

$$Q_3^{(I,J)}(v) = \widehat{Q}_3^{(I,J)} \frac{\lambda_I \lambda_J \acute{A}_I \acute{A}_J + \kappa_I \kappa_J A_I A_J}{\kappa_I \kappa_J A_I A_J} \tag{4.9}$$

Then (4.8) reduces to the condition we would take for the five-dimensional case ($\lambda_I = \lambda_J = 0$)

$$\widehat{Q}_3^{(I,J)} \geq \left(Q_1^{(I)} Q_2^{(J)} + Q_2^{(I)} Q_1^{(J)} \right) \frac{\kappa_I \kappa_J}{8} \tag{4.10}$$

One should also verify that the global condition (3.15) is satisfied by numerically examining the space between the different supersheets for specific choices of the functions $A_I(v)$. We partially perform this analysis later on and find there are areas of the parameter space of solutions that is satisfied. In general, because of the correspondence to the five-dimensional case, if the supersheets are well separated and the oscillations along v are small we expect the solution to be regular.

The asymptotic charges of the solution in addition to being the sum of the singe-centered pieces they will also get contributions from the interaction terms. The asymptotic electric charges are

$$Q_{1,\infty} = \sum_I Q_1^{(I)} \, , \, Q_{2,\infty} = \sum_I Q_2^{(I)} \, , \, Q_{3,\infty} = \sum_I Q_3^{(I)} + 2 \sum_{I<J} Q_3^{(I,J)} \tag{4.11}$$

and by expanding ω we get

$$\omega \sim \frac{1}{r^2} \left(\sum_I J^{(I)} + \sum_{I<J} J^{(I,J)} \right) \tag{4.12}$$

where

$$\begin{aligned} J^{(I)} &= \left(\kappa_I A_I^2 (Q_1^{(I)} + Q_2^{(I)}) + \kappa_I Q_1^{(I)} Q_2^{(I)} \right) sin^2\theta d\psi + \kappa_I Q_1^{(I)} Q_2^{(I)} cos^2\theta d\phi + \\ &+ \frac{1}{2} (Q_1^{(I)} + Q_2^{(I)}) \lambda_I A_I \acute{A}_I sin(2\theta) d\theta \\ J^{(I,J)} &= \left(Q_1^{(I)} Q_2^{(J)} + Q_2^{(I)} Q_1^{(J)} \right) \kappa_J \left(sin^2\theta d\psi + cos^2\theta d\phi \right) \end{aligned} \tag{4.13}$$

The contributions to the angular momentum that come from the interaction pieces neither depend on $\dot{A}$ nor do they have a $d\theta$ component. Thus the interaction terms in the asymptotic charges for multi-centered breathing supersheets are the same with those for solutions with trivial reduction to five dimensions. It will be interesting to examine whether this holds when we include the third dipole charge i.e. $\beta \neq 0$.

Having fully described the solution there is an interesting coincidence limit where all the supersheets become identical

$$A_I \to A \, , \, \lambda_I \to \lambda \, , \, \kappa_I \to \kappa \, , \, Q_i^{(I)} \to Q_i \, , \, Q_3^{(I,J)} \to Q_3 \tag{4.14}$$

for all the N centers of the solution and for $i = 1, 2, 3$. Then we obtain the single-centered solution of section 3 and its asymptotic charges with

$$Q_1 \to N Q_1 \, , \, Q_2 \to N Q_2 \, , \, Q_3 \to N^2 Q_3 \tag{4.15}$$

4.3 Touching, Crossing & Regularity

Although so far we have strictly imposed the condition $A_I < A_J \quad \forall v \in [0, L]$, the functions describing the solution are regular at the limit $A_I \to A_J$. The single-centered terms $H^{(I)}$, $\mathcal{F}^{(I)}$,

$\omega^{(I)}$ and the interaction terms $\mathcal{F}^{(I,J)}$, $\omega_1^{(I,J)}$ are trivially regular at this limit. For the terms appearing in $\omega_2^{(I,J)}$ the functions $G_1^{(I,J)}$ and $G_2^{(I,J)}$ are regular while $L_1^{(I,J)}$ and $L_2^{(I,J)}$ are singular. However one can observe from $\omega_2^{(I,J)}$ in (4.4) that at the limit $A_I \to A_J$ the $d\phi$ and $d\zeta$ components factorize and the quantity $L_1^{(I,J)} + L_2^{(I,J)}$ is regular as well. Thus it seems that since supersheets can be realized as a collection of different v-slices we can have different supersheets touching or crossing (fig.2) over each other at specific values of $v = v_2$ such that $A_I(\lambda_I v_2) = A_J(\lambda_J v_2)$.

For touching supersheets we should by definition have,

$$A_I(\lambda_I v_2) = A_J(\lambda_J v_2) \quad , \quad \dot{A}_I(\lambda_I v_2) = \dot{A}_J(\lambda_J v_2) \tag{4.16}$$

Then continuity of the solution requires that taking the limit (4.16) on the result (4.4), (4.6) should match the result of the smearing integral for $v = v_2$ where (4.16) holds before smearing. Then one gets that the helical winding numbers of the two supersheets should match i.e. $\kappa_I = \kappa_J$. Overall the conditions for two supersheets touching at $v = v_2$ are

$$\kappa_I = \kappa_J \, , \, A_I(\lambda_I v_2) = A_J(\lambda_J v_2) \, , \, \dot{A}_I(\lambda_I v_2) = \dot{A}_J(\lambda_J v_2) \tag{4.17}$$

The somewhat notorious case of supersheets crossing over each other such that $A_I(\lambda_I v_2) = A_J(\lambda_J v_2)$ needs some additional attention, as the ordering of the supersheets changes. As we mentioned at the end of section 4.1 not only the functions $\mathcal{F}^{(I,J)}$ and $\omega_2^{(I<J)}$ describing the interactions between different supersheets are not symmetric under $I \leftrightarrow J$, but also the ordering of the supersheets matters in calculating the integrals. Reminding ourselves that our solution is a collection of different constant v slices the previous issue could easily be resolved. One would have to calculate the smearing integrals of the interaction at two different areas of the coordinate v. For $v < v_2$ we have $A_I < A_J$ and the result would be the functions $\mathcal{F}^{(I,J)}$ and $\omega_2^{(I,J)}$ as given by (4.4), (4.6). For $v > v_2$ we would have $A_I > A_J$ and thus

$$\begin{aligned} \widetilde{\mathcal{F}}^{(I,J)} &= \mathcal{F}^{(J,I)} \\ \widetilde{\omega}_2^{(I,J)} &= \omega_2^{(J,I)} \end{aligned} \tag{4.18}$$

Then we should at least require that the functions describing the supersheets are continuous at the crossing point $v = v_2$, which means we should demand

$$\begin{aligned} \lim_{v \to v_2} \left(\mathcal{F}^{(I,J)} - \widetilde{\mathcal{F}}^{(I,J)} \right) &= 0 \\ \lim_{v \to v_2} \left(\omega_2^{(I,J)} - \widetilde{\omega}_2^{(I,J)} \right) &= 0 \end{aligned} \tag{4.19}$$

Using (4.18) we find for the difference of the functions

$$
\begin{aligned}
&\lim_{v\to v_2}\left(\mathcal{F}^{(I,J)}-\widetilde{\mathcal{F}}^{(I,J)}\right)=4\frac{Q_3^{(J,I)}(v_2)-Q_3^{(I,J)}(v_2)}{\Sigma_I}\\
&\lim_{v\to v_2}\left(\omega_2^{(I,J)}-\widetilde{\omega}_2^{(I,J)}\right)=\lim_{v\to v_2}\left(Q_1^{(I)}Q_2^{(J)}+Q_2^{(I)}Q_1^{(J)}\right)\cdot\\
&\cdot\Bigg(\left(-\left(G_1^{(I,J)}+G_2^{(J,I)}\right)\kappa_I+\left(G_2^{(I,J)}+G_1^{(J,I)}\right)\kappa_J\right)d\psi+\\
&+\left(-\frac{\acute{A}_I}{A_I\eta}\left(G_1^{(I,J)}+G_2^{(J,I)}\right)\lambda_I+\frac{\acute{A}_J}{A_I\eta}\left(G_2^{(I,J)}+G_1^{(J,I)}\right)\lambda_J\right)d\eta\Bigg)
\end{aligned}
\tag{4.20}
$$

Thus taking the limit $v\to v_2$, for (4.19) to hold we need

$$
Q_3^{(I,J)}(v_2)=Q_3^{(J,I)}(v_2)\,,\;\kappa_I=\kappa_J\,,\;\dot{A}_I(\lambda_I v_2)=\dot{A}_J(\lambda_J v_2)\,,\;A_I(\lambda_I v_2)=A_J(\lambda_J v_2)
\tag{4.21}
$$

The conditions (4.21) suggest that the supersheets can only cross through a point at which they tangentially touch each other. It is interesting to observe that both crossing and touching require the helical winding numbers κ_I, κ_J to be the same. In both cases the requirement of a local condition (continuity) gives a constraint on the global parameters κ. This constraint (along with $\dot{A}_I=\dot{A}_J$ for crossing) can be understood as if for the supersheets to touch or cross, the superthreads that consist them should at the touching or crossing point $v=v_2$ realize each others as constituents of the same single-centered supersheet. Another way of realizing the constraints (4.17), (4.21) is through the angular momentum of the supersheets (4.12), (4.13). The parameters κ_I generate the ψ, ϕ components of the angular momentum and $\dot{A}_I$ the θ one. Thus for the supersheets to touch or cross regularity requires that at the point of touching they should rotate in the same manner.

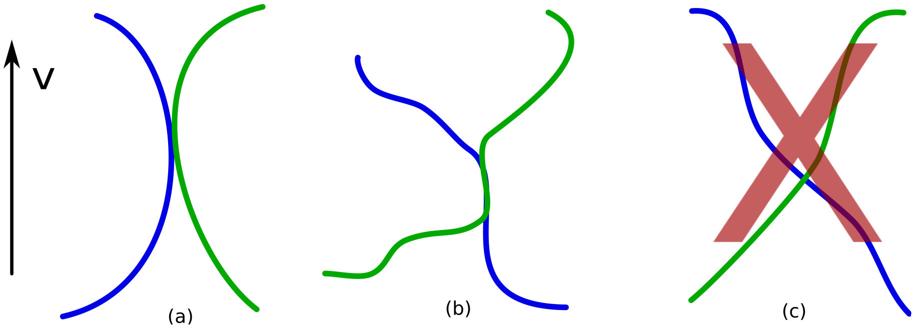

Figure 2: *Sections of different supersheets (blue & green): (a) touching supersheets, (b) supersheets crossing by touching tangentially, (c) supersheets cannot cross without touching tangentially.*

One additional remark is that because the five dimensional bubble equations are encoded in the ordering of the supersheets and since at a touching or crossing point the ordering becomes degenerate, the constraints (4.17), (4.21) are basically the six-dimensional conditions for the absence of Dirac strings when different supersheets touch or cross.

4.4 Numerics on Global Regularity Conditions

So far we have examined the case of well separated multi-centered supersheets as well as the case when they touch or cross. In our analysis we mainly focused in the local regularity conditions that these solutions have to satisfy. However one should also check the global constraints (3.14), (3.15) which come from the absence of closed timelike curves. Here by considering specific examples of two concentric supersheets we perform a partial numerical analysis of these constraints and observe that at the usual areas of danger, our solutions pass the test. We will focus in the area between the supersheets and examine the phase space of solutions as the two supersheets approach or as we vary the parameters κ_1, κ_2. Regarding (3.15) we will examine the $d\psi^2$ part of it, which matches the five dimensional global regularity condition [7]. In all of the cases we will have a non breathing supersheet of constant radius A_1 and we choose

$$Q_1^{(1)} = Q_2^{(1)} = Q_1^{(2)} = Q_2^{(2)} = 1\,,\; Q_3^{(1)} = Q_3^{(2)} = Q_3^{(21)} = 50\,,\; \theta = \frac{\pi}{2} \tag{4.22}$$

For distinct or touching supersheets we will choose

$$A_2 = 6 + sinv \tag{4.23}$$

which means that $0 < A_1 \leq 5$ with the supersheets touching for $A_1 = 5$. For $A_1 < 5$ we will examine the area for $v = \frac{3\pi}{2}$ where the supersheets A_1 and A_2 are closest to each other and we will choose the radial distance to be in the middle of the two supersheets $r = \frac{5+A_1}{2}$. The results are shown in figures (3(a)), (3(b)), (4) in terms of contour plots of (3.15). In fig.(3(a)) we have chosen $A_1 = 2$ and corresponds to the case where the supersheets are well separated. We see that there is enough parameter space for κ_1, κ_2 before closed timelike curves appear. In fig.(3(b)) we have $A_1 = 4.9$ and the allowed parameter space for κ_1, κ_2 is significantly smaller. This is displayed better in fig.(4) where we have set $\kappa_1 = \kappa_2$ (the condition for touching) and observe how the allowed values decrease as the supersheets approach.

For touching supersheets we have $A_1 = 5$ and $\kappa_1 = \kappa_2 = \kappa$. We set $v = \frac{3\pi}{2} + 0.1$ and examine the area between the two supersheets near the touching point as we vary κ and the radius r. The results are displayed in fig.(5). Once again we see there are ample of values for κ so that (3.15) is satisfied.

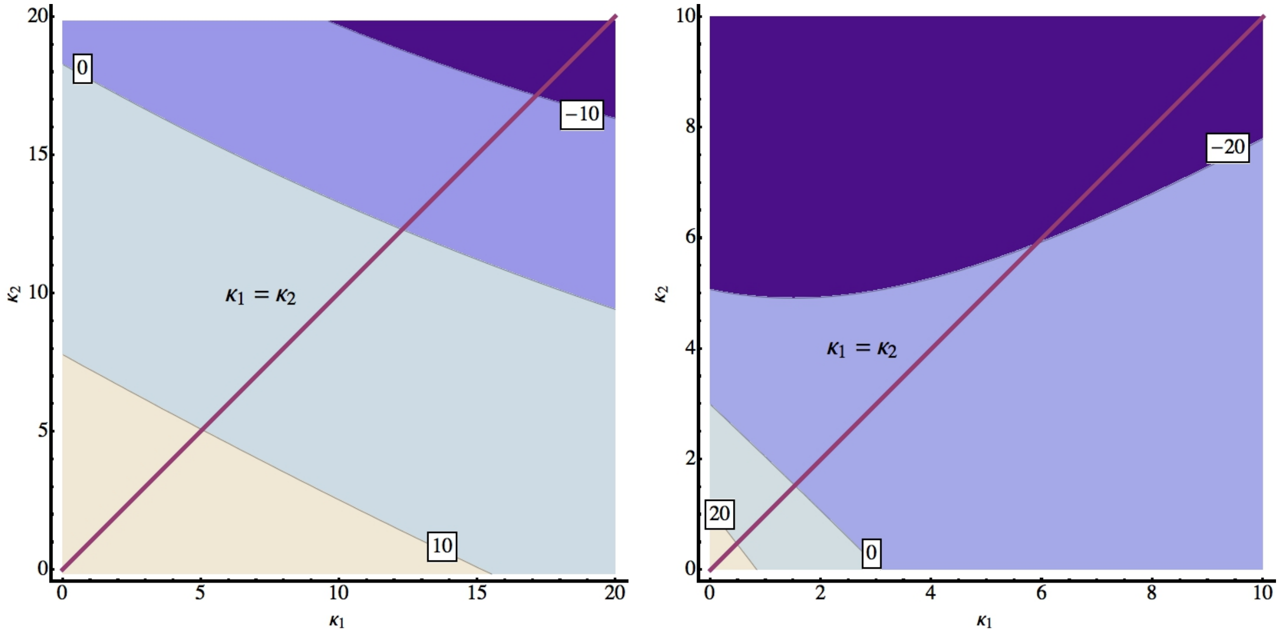

(a) $A_1 = 2$ Well separated supersheets

(b) $A_1 = 4.9$ Supersheets close to each other

Figure 3: *Contour plot of the* $d\psi^2$ *component of (3.15) for* $\theta = \frac{\pi}{2}$ *shows the allowed values of* κ_1, κ_2 *for separated supersheets in the middle of the area between them. The allowed values reduce as the supersheets approach.*

For crossing supersheets we choose

$$A_1 = 5\,,\; A_2 = 5 + \left(\sin\left(v + \frac{\pi}{2}\right)\right)^3 \tag{4.24}$$

The function A_2 has inflection points for $v = (2n+1)\frac{\pi}{2}$, where $n \in \mathbb{Z}$. At these points $A_1 = A_2$ and that's when the two supersheets cross. As in the case of touching supersheets we are going to choose $v = \frac{3\pi}{2} + 0.1$, so that we are near the crossing point, and examine the area between A_1 and A_2. As we observe from fig.(6) there allowed values of κ from (3.15) and thus the solution exists.

The condition (3.14) is trivially satisfied in the areas we examined so far. Examining (3.14) near the origin we also need (3.16), (4.8). Also from examining (3.15) near the supersheets when $\dot{A}_I = 0$ we additionally get (3.21). All of these conditions (3.16), (4.8), (3.21) set finite upper bounds to the values of κ_1, κ_2. Upper bounds to the values of κ_1, κ_2 have also been found in the numerical analysis presented in this section. Thus the conditions (3.16), (4.8), (3.21 together with examining (3.15) in the area between the supersheets will have a common set of allowed values for κ_1, κ_2.

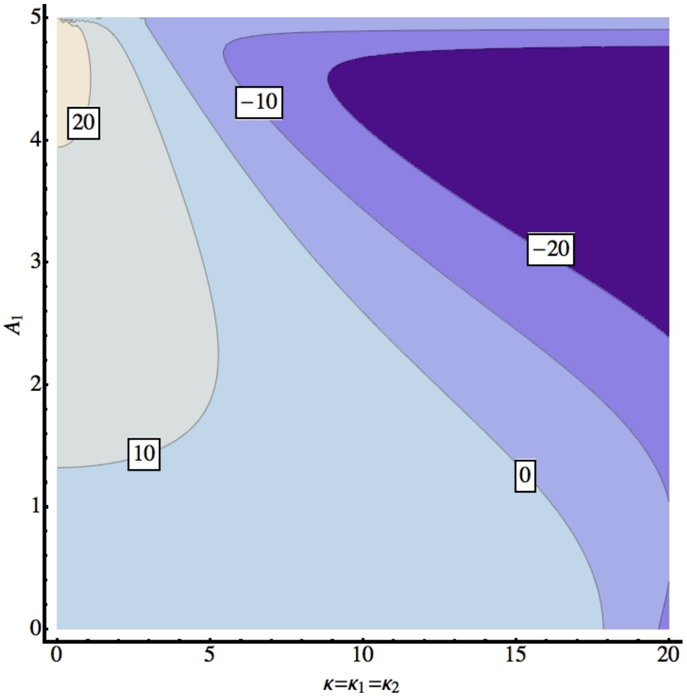

Figure 4: *Contour plot of the* $d\psi^2$ *component of (3.15) for* $\theta = \frac{\pi}{2}$ *in the middle of the area between two supersheets with same helical mode* κ. *The allowed values of* κ *reduce as the supersheets approach.*

5 Suggestions on the Addition of KKM

The geometries we have studied so far are restricted to setting $\beta = 0$ and hence there is no third dipole charge. The addition of β is needed to construct not only generic black hole solutions, but also the superstratum. Here we use the results of this paper to argue about certain aspects of the solution that include β [3]. We find that our arguments are consistent with previous analysis regarding the superstratum [27].

The difficulty arises because the BPS equation [2] for β is non-linear

$$\mathcal{D}\beta = *_4\mathcal{D}\beta \tag{5.1}$$

where

$$D\Phi = \tilde{d}\Phi - \beta \wedge \dot{\Phi} \tag{5.2}$$

---

[3] Geometries with all three electric and dipole magnetic charges (they have $\beta \neq 0$ but still $\dot{\beta} = 0$) have been constructed in [33] for a Kähler base space. In contrast to five dimensions, in six dimensions the BPS conditions do not require the base space to be hyper-Kähler [2, 3] and indeed the more general solutions we are after may require a more general class of metrics. However it is still interesting to examine which genuinely six-dimensional geometries can be constructed with a hyper-Kähler base.

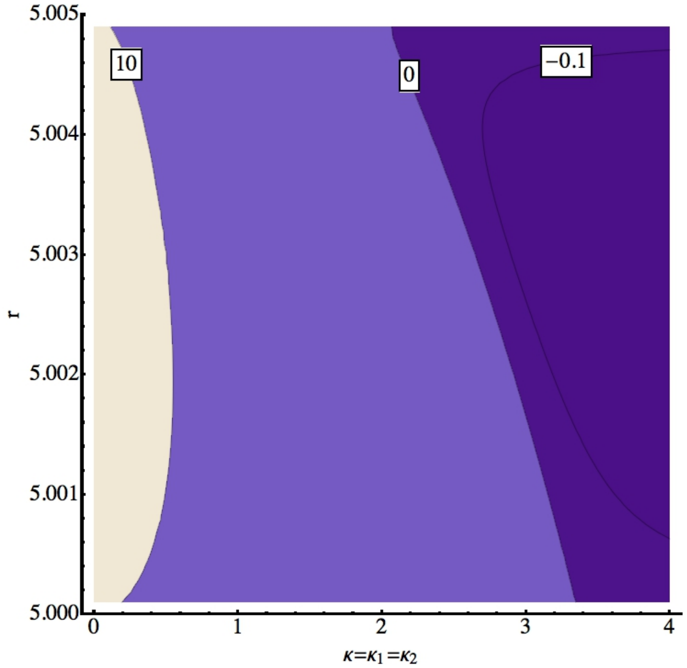

Figure 5: *For touching supersheets there are allowed values of κ for all radial distances r in the area between them next to the touching point.*

and $\tilde{d}$ is the exterior derivative with respect to the four-dimensional base space. When β is v independent (5.1) becomes linear and reduces to the equation know from linearity in five dimensions

$$\tilde{d}\beta = *_4\tilde{d}\beta \tag{5.3}$$

In section 3.2 we observed that because of the periodicity of v, there should be values of $v = v_1$ such that $\dot{A}(\lambda v_1) = 0$. At these points our solution directly reduces to the non-breathing supersheet which is essentially five-dimensional. Thus for any generic genuinely six-dimensional solution there are points along the compactification circle that the solutions looks five-dimensional. Consequently, we should be able to explore six-dimensional solutions by adding appropriate perturbations around the points $v = v_1$ to already known geometries from five dimensions. This should be allowed based on the superposition of breathing and helical modes we constructed in section 3.2. At $v = v_1$ we should simultaneously have

$$\dot{A}(v_1) = 0\,,\ \dot{\beta}(v_1) = 0 \tag{5.4}$$

with $A(v)$ representing the radius of the profile in the four-dimensional base metric.Thus by expanding around $v = v_1$, β should at least have similar linear order dependence on v with A.

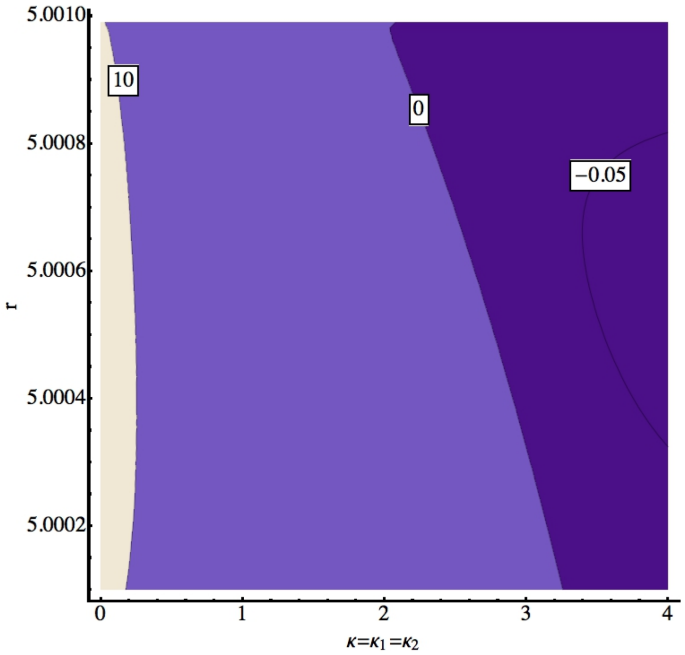

Figure 6: *For crossing supersheets there are allowed values of κ for all radial distances r in the area between them next to the crossing point.*

The superstratum, since it is a smooth geometry, is expected to be much more constrained compared to generic black geometries and one would have to add appropriate perturbations in a very precise manner. Indeed, the only known D1-D5 single-centered geometry that is smooth in six dimensions and can be reduced to five is the supertube. The supertube carries D1, D5 electric charges and KKM dipole charge. The superstratum is expected to have all three electric (D1-D5-P) and magnetic dipole (d1-d5-KKM) charges. Thus for $v = v_1$ the superstratum should look exactly like a supertube aligned along the v direction and because of the smoothness of the solution we should simultaneously have

$$\begin{aligned} &\dot{A}(v_1) = 0\,,\ \dot{\beta}(v_1) = 0 \\ &P(v_1) = 0\,,\ d1(v_1) = d5(v_1) = 0 \end{aligned} \tag{5.5}$$

The additional requirement on the charges of the object is consistent with the supersymmetry analysis in [27]. The D1-D5 system is being placed along the v direction and is being given momentum P vertically with respect to the branes This gives a system with charges $Q_1 = Q_{D1}$, $Q_2 = Q_{D5}$ and angular momentum $J = P$. To generate dipole charge and momentum along v one gives a tilt of angle α to the D1-D5 system with respect to the v direction. Then

$$d1 = Q_{D1} sin\alpha\,, d5 = Q_{D5} sin\alpha\,,\ P_v = P sin\alpha \tag{5.6}$$

Then, the conditions on the charges in (5.5) can be simultaneously satisfied provided the tilting angle α is a function of v such that

$$\alpha = \alpha(v)\,,\ \alpha(v_1) = n\pi \tag{5.7}$$

where n is an integer. The dependence of the tilting angle with respect to v is essential part of the second supertube transition [27] required to generate the superstratum.

6 Conclusions

Minimal ungauged $\mathcal{N} = 1$ supergravity in six dimensions coupled to one anti-self-dual tensor multiplet can be reduced to five-dimensional $\mathcal{N} = 2$ ungauged supergravity coupled to two vector multiplets. In recent work [2] the BPS equations of the six-dimensional theory were shown to admit a linear structure. This allows new classes of black hole and microstate geometries to be constructed that are part of the D1-D5 system and have $AdS_3 \times S^3$ asymptotics. In general these geometries would have three electric (D1-D5-P) and three dipole magnetic charges (d1-d5-KKM).

Here we extended the results of previous work [1] to describe multi-centered solutions with D1-D5-P electric charges and d1-d5 magnetic dipoles, which have a non-trivial dependence on the compactification direction. The supersheet profile functions were chosen so that they are the product of a helical mode and an arbitrary breathing mode. Then we saw that after smearing the resulting supersheet is basically the superposition of two separate smeared supersheets, one with a straight breathing mode and one with a helical mode but with no v dependence. For the multi-centered case the supersheets interact in pairs and we observed that the absence of integrability conditions is encoded as a lack of symmetry in exchanging the two centers in the functions describing the interaction. Before smearing the integrands are symmetric in exchanging the centers, but while performing the integral one has to choose an order to decide which poles are within the unit circle. The asymptotic charges get contributions from the interaction terms between the supersheets, but interestingly enough these extra terms do not get affected by the non-trivial dependence along the compactification direction. Thus the contribution of the interaction to the asymptotic charges is essentially five-dimensional.

A new feature is that different supersheets can under certain conditions touch and cross through each other without the occurrence of closed timelike curves. The local regularity conditions (originating from the absence of Dirac-strings in five dimensions) require that the supersheets come in contact tangentially and also have the same helical mode windings κ_I. These conditions essentially guarantee that the superthreads making the two supersheets can at the point of contact realize themselves as constituents of a single supersheet. This feature is a consequence of the fact that our solutions can be realized as a sequence of different slices of constant v and it would be interesting to examine whether such a feature holds to more general six-dimensional solutions with $\beta \neq 0$.

Another interesting aspect of the solutions is that because the direction v is periodic there are values v_1 of v where the first derivative of the radius of the four-dimensional profile $A(v)$ vanishes and thus the solution looks five-dimensional. This, together with the superposition of breathing and helical modes, gives hope that one will be able to add perturbative modes on already known five-dimensional solutions to generate a richer class of solutions. We should note however that when $\beta \neq 0$ there might be a wider class of solutions such that there is no superposition between helical and breathing modes.

All in all, this paper by considering a specific class of examples reveals some of the characteristics of six-dimensional D1-D5-P geometries and to the best of our knowledge the first example of a multi-centered case. The expectation is that the results of our analysis will help us find more general classes of geometries, the conjectured superstratum, construct multi-centered black and microstate systems as well as their non-supersymmetric analogs. We leave the exploration of these more general geometries for the future.

Acknowledgements

I would like to thank Nick Warner for very valuable conversations and Ben Niehoff for helpful discussions during the early stages of this project. This work is supported in part by DOE grant DE-FG03-84ER-40168. OV would like to thank the USC Dana and David Dornsife College of Letters, Arts and Sciences for support through the College Doctoral Fellowship.

References

[1] B. E. Niehoff, O. Vasilakis and N. P. Warner, “Multi-Superthreads and Supersheets,” arXiv:1203.1348 [hep-th].

[2] I. Bena, S. Giusto, M. Shigemori and N. P. Warner, “Supersymmetric Solutions in Six Dimensions: A Linear Structure,” arXiv:1110.2781 [hep-th].

[3] J. B. Gutowski, D. Martelli and H. S. Reall, “All supersymmetric solutions of minimal supergravity in six dimensions,” Class. Quant. Grav. **20**, 5049 (2003) [arXiv:hep-th/0306235].

[4] M. Cariglia and O. A. P. Mac Conamhna, “The general form of supersymmetric solutions of N = (1,0) U(1) and SU(2) gauged supergravities in six dimensions,” Class. Quant. Grav. **21**, 3171 (2004) [arXiv:hep-th/0402055].

[5] I. Bena and N. P. Warner, "One ring to rule them all ... and in the darkness bind them?," Adv. Theor. Math. Phys. **9**, 667 (2005) [arXiv:hep-th/0408106].

[6] J. P. Gauntlett, J. B. Gutowski, C. M. Hull, S. Pakis and H. S. Reall, "All supersymmetric solutions of minimal supergravity in five- dimensions," Class. Quant. Grav. **20**, 4587 (2003) [hep-th/0209114].

[7] I. Bena and N. P. Warner, "Black holes, black rings and their microstates," Lect. Notes Phys. **755**, 1 (2008) [arXiv:hep-th/0701216].

[8] P. Berglund, E. G. Gimon and T. S. Levi, "Supergravity microstates for BPS black holes and black rings," JHEP **0606**, 007 (2006) [hep-th/0505167].

[9] I. Bena, S. Giusto, C. Ruef and N. P. Warner, "Supergravity Solutions from Floating Branes," JHEP **1003**, 047 (2010) [arXiv:0910.1860 [hep-th]].

[10] K. Goldstein and S. Katmadas, "Almost BPS black holes," JHEP **0905**, 058 (2009) [arXiv:0812.4183 [hep-th]].

[11] I. Bena, G. Dall'Agata, S. Giusto, C. Ruef and N. P. Warner, "Non-BPS Black Rings and Black Holes in Taub-NUT," JHEP **0906**, 015 (2009) [arXiv:0902.4526 [hep-th]].

[12] I. Bena, S. Giusto, C. Ruef and N. P. Warner, "Multi-Center non-BPS Black Holes: the Solution," JHEP **0911**, 032 (2009) [arXiv:0908.2121 [hep-th]].

[13] O. Vasilakis and N. P. Warner, "Mind the Gap: Supersymmetry Breaking in Scaling, Microstate Geometries," JHEP **1110**, 006 (2011) [arXiv:1104.2641 [hep-th]].

[14] N. Bobev, B. Niehoff and N. P. Warner, "Hair in the Back of a Throat: Non-Supersymmetric Multi-Center Solutions from Káhler Manifolds," JHEP **1110**, 149 (2011) [arXiv:1103.0520 [hep-th]].

[15] N. Bobev and C. Ruef, "The Nuts and Bolts of Einstein-Maxwell Solutions," JHEP **1001**, 124 (2010) [arXiv:0912.0010 [hep-th]].

[16] G. Dall'Agata, S. Giusto and C. Ruef, "U-duality and non-BPS solutions," JHEP **1102**, 074 (2011) [arXiv:1012.4803 [hep-th]].

[17] G. Bossard and C. Ruef, "Interacting non-BPS black holes," Gen. Rel. Grav. **44**, 21 (2012) [arXiv:1106.5806 [hep-th]].

[18] O. Lunin and S. D. Mathur, "AdS/CFT duality and the black hole information paradox," Nucl. Phys. B **623**, 342 (2002) [arXiv:hep-th/0109154].

[19] O. Lunin, J. M. Maldacena and L. Maoz, "Gravity solutions for the D1-D5 system with angular momentum," arXiv:hep-th/0212210.

[20] S. D. Mathur, "The fuzzball proposal for black holes: An elementary review," Fortsch. Phys. **53**, 793 (2005) [arXiv:hep-th/0502050].

[21] B. D. Chowdhury and A. Virmani, "Modave Lectures on Fuzzballs and Emission from the D1-D5 System," arXiv:1001.1444 [hep-th].

[22] S. D. Mathur, "Fuzzballs and the information paradox: a summary and conjectures," arXiv:0810.4525 [hep-th].

[23] V. Balasubramanian, J. de Boer, S. El-Showk and I. Messamah, "Black Holes as Effective Geometries," Class. Quant. Grav. **25**, 214004 (2008) [arXiv:0811.0263 [hep-th]].

[24] K. Skenderis and M. Taylor, "The fuzzball proposal for black holes," Phys. Rept. **467**, 117 (2008) [arXiv:0804.0552 [hep-th]].

[25] J. de Boer and M. Shigemori, "Exotic branes and non-geometric backgrounds," Phys. Rev. Lett. **104**, 251603 (2010) [arXiv:1004.2521 [hep-th]].

[26] J. de Boer and M. Shigemori, "Exotic Branes in String Theory," arXiv:1209.6056 [hep-th].

[27] I. Bena, J. de Boer, M. Shigemori and N. P. Warner, "Double, Double Supertube Bubble," JHEP **1110**, 116 (2011) [arXiv:1107.2650 [hep-th]].

[28] S. Giusto and R. Russo, "Perturbative superstrata," arXiv:1211.1957 [hep-th].

[29] I. Bena and P. Kraus, "Three charge supertubes and black hole hair," Phys. Rev. D **70**, 046003 (2004) [hep-th/0402144].

[30] I. Bena, "Splitting hairs of the three charge black hole," Phys. Rev. D **70**, 105018 (2004) [hep-th/0404073].

[31] I. Bena, P. Kraus and N. P. Warner, "Black rings in Taub-NUT," Phys. Rev. D **72**, 084019 (2005) [hep-th/0504142].

[32] O. Vasilakis, "Bubbling the Newly Grown Black Ring Hair," JHEP **1205**, 033 (2012) [arXiv:1202.1819 [hep-th]].

[33] N. Bobev, B. E. Niehoff and N. P. Warner, "New Supersymmetric Bubbles on $AdS_3 x S^3$," JHEP **1210**, 013 (2012) [arXiv:1204.1972 [hep-th]].